

Structural Characterization of α -Zein

FRANK A. MOMANY,* DAVID J. SESSA, JOHN W. LAWTON, GORDON W. SELLING,
 SHARON A. H. HAMAKER, AND JULIOUS L. WILLETT

Plant Polymer Research Unit, MWA, National Center for Agricultural Utilization Research,
 Agricultural Research Service, U.S. Department of Agriculture, 1815 North University Street,
 Peoria, Illinois 61604

A variety of published physical measurements, computational algorithms, and structural modeling methods have been used to create a molecular model of 19 kDa α -zein (Z19). Zeins are water-insoluble storage proteins found in corn protein bodies. Analyses of the protein sequence using probability algorithms, structural studies by circular dichroism, infrared spectroscopy, small-angle X-ray scattering (SAXS), light scattering, proton exchange, NMR, and optical rotatory dispersion experiments suggest that Z19 has ~35–60% helical character, made up of nine helical segments of about 20 amino acids with glutamine-rich “turns” or “loops”. SAXS and light-scattering experiments suggest that in alcohol/water mixtures α -zein exists as an oblong structure with an axial ratio of ~6:1. Furthermore, ultracentrifugation, birefringence, dielectric, and viscosity studies indicate that α -zein behaves as an asymmetric particle with an axial ratio of from 7:1 to 28:1. Published models of α -zein to date have not been consistent with the experimental data, and for this reason the structure was re-examined using molecular mechanics and dynamics simulations creating a new three-dimensional (3D) structure for Z19. From the amino acid sequence and probability algorithms this analysis suggested that α -zein has coiled-coil tendencies resulting in α -helices with about four residues per turn in the central helical sections with the nonpolar residue side chains forming a hydrophobic face inside a triple superhelix. The nine helical segments of the 19 kDa protein were modeled into three sets of three interacting coiled-coil helices with segments positioned end to end. The resulting structure lengthens with the addition of the N- and C-terminal sections, to give an axial ratio of ~6 or 7:1 in agreement with recent experiments. The natural carotenoid, lutein, is found to fit into the core of the triple-helical segments and help stabilize the configuration. Molecular dynamics simulations with explicit methanol/water molecules as solvent have been carried out to refine the 3D structure.

KEYWORDS: α -Zein; 3D structure; storage proteins

INTRODUCTION

Alcohol-soluble storage proteins of corn/maize seeds are collectively known as zeins. The function of these proteins is apparently to store nitrogen for the developing seed; however, their polymeric uses are of considerable interest (1). The four main types of zein (denoted α , β , γ , and δ) are classified according to their solubility properties, and the α -zeins of interest here display high hydrophobic properties. Although generally found as disulfide-bridged dimers, the individual α -zeins have molecular masses of 19 and 22 kDa, the size difference being from an amino acid insertion in the C-terminal region of the 22 kDa form.

Studies bearing on the α -zein conformation or three-dimensional (3D) structure in solution have suggested a 3D structure with high axial ratio (2–5). In the 1930s, Williams and Watson (2) described an axial ratio of 25:1 in 60% aqueous ethanol. Elliott and Williams (3) and Foster and Edsall (4)

determined a shape resembling a prolate ellipsoid with axial ratios of ~7:1 and 15:1, respectively. In the 1940s, Oncley et al. (5) determined an axial ratio of ~9:1 in 73% aqueous ethanol from dielectric studies. The 1950–1970s produced studies of the helical content of zein (6, 7) by optical rotation, resulting in helix content in ethanol/water of 35–60%. Most early studies were made on preparations that were heterogeneous, having molecular weights considerably larger than that of an individual α -zein molecule. For this reason they must be considered mixtures or dimer complexes of different zeins.

Several models have been proposed for the 3D structure of α -zein, including one composed of a series of antiparallel helices clustered within a distorted cylinder (8). Argus et al. (8) utilized helical propensities from prediction algorithms and optical rotation studies, as well as hydrophobicity profiles to conclude that the structure was composed of helix clusters with an axial ratio of ~2:1. Garrett et al. (9) developed a model based on hydrophobic membrane propensities and helical “wheels.” They suggested that pairs of repeats formed antiparallel α -helical hairpins and were arranged in a hexagonal net. Tatham et al.

* Author to whom correspondence should be addressed (e-mail momanyfa@ncaur.usda.gov).

(10) have concluded from X-ray scattering and viscosity studies that α -zein in solution is a relatively rigid asymmetric particle with a diameter between 0.7 and 1.5 nm and length of ~ 15 nm by small-angle X-ray scattering (SAXS) and 24 nm by viscosity. More recently, Matsushima et al. (11), using SAXS, proposed that α -zein could be represented by an elongated prism-like shape with an approximate axial ratio of 6:1. Most recently, Bugs et al. (12) proposed a model in which two antiparallel α -helices were created from coiled-coils to form a superhelical conformation. Their (12) structure for α -zein contained 70% helix, 13% turns, and the remainder in a loosely organized extended random coil. The result was a structure with an axial ratio of $\sim 4:1$ in only fair agreement with experimental axial ratios. Also in 2004, Forato et al. (13) created a hairpin turn model with sections of helix spaced rather randomly with random coil sections between the helices and the whole structure folded back upon itself. This model (13) appears to allow for fast N-H to N-D exchange as measured by ^1H NMR and results in a maximum length of 12–13 nm and transverse dimensions from 2 to 4 nm.

In the work presented here a totally new model for the solution structure of α -zein is proposed that agrees with the dimensions arrived at by various experimental methods and goes on to explain the binding of lutein and the difficulty of removing lutein from α -zein solutions.

COMPUTATIONAL METHODS

All calculations were carried out using the AMBER (14) force field. The AMBER force field resides in the InsightII/Discover software from Accelrys Inc. (15). The dielectric constant is retained at 1 with the electrostatic nonbonded 1–4 terms scaled by 0.5. Partial atomic charges for the amino acids are those found in the AMBER program (14). Empirical energy minimization is carried out to a gradient of less than ~ 0.001 kcal/mol. During molecular dynamics, integration is numerically carried out using the Verlet algorithm and trajectories initiated by assigning velocity components randomly selected from a thermal distribution at the appropriate temperature to the atoms. Calculations were carried out at several temperatures controlled by a weak coupling to a temperature bath. Time steps of 1 fs were used to calculate velocities, but results are stored for examination at picosecond (ps) intervals. Equilibrium times was $\sim 1/10$ of the total simulation time. Explicit hydrogen atoms were included in all calculations, and both heavy atoms and hydrogen atoms are flexible on all molecules. TIP3P water potentials and charges are used without constraints, similarly for the methanol molecules used as solvent. The solvent was a mixture of methanol and water at ($\sim 90/10\%$), respectively. This ratio of methanol/water is found experimentally to produce clear solutions of Z19. The solvent was computationally added as layers on the protein surface and extensively energy minimized to prevent boiling off upon application of molecular dynamics. Coiled-coil probability algorithms were used (16) as were standard helix probabilities available in InsightII (15).

RESULTS

The N-terminal segment after the signal peptide (residues 22–57 of a 19 kDa zein precursor, denoted locus ZIZM92) was first carried through a series of molecular dynamics simulations in methanol/water at (90/10%) as solvent. There is no propensity for helix formation in this section of the protein, as predicted by helical probability algorithms. The folding pattern resulting from these simulations is shown in Figure 1. The resulting compact structure has some favorable properties thought to be important. For example, the cysteine residue (C27 or C6 in the renumbered sequence starting at residue 22) is exposed on the surface and so is available to form a disulfide bridge with the cysteine residue of the Z22 protein, creating the naturally found dimer. The N and C termini are close to one another, a result of a large chain reversal in the middle of the segment and the

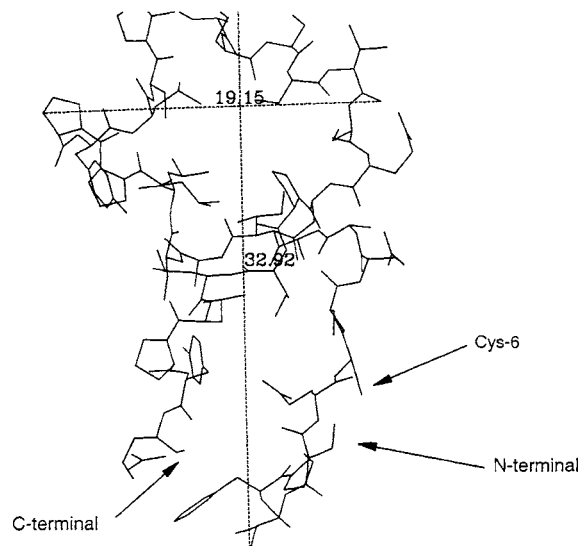


Figure 1. Stick model representation of the N-terminal segment of Z19. Distances shown by dotted lines are in angstroms.

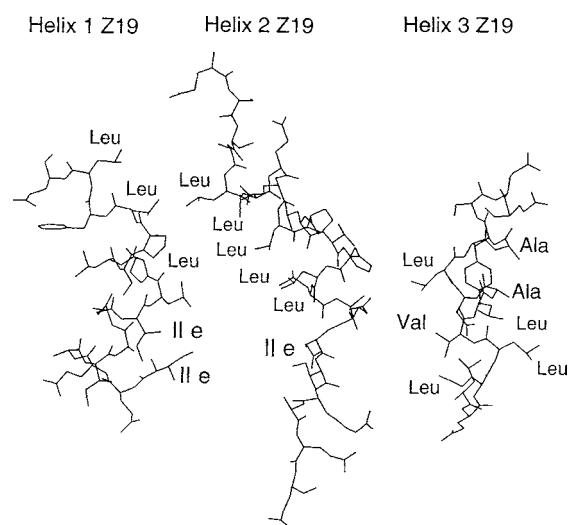


Figure 2. Stick model representation of helix segments 1–3 showing the Leu, Ile, Ala, and Val residues.

disruption of secondary structure as a result of the nine proline residues in this segment. The size of this fragment is ~ 2 nm wide by ~ 3 nm long and is generally made up of random coil and β -sheet secondary structure. This segment is not stabilized by any major secondary structure and so possibly unravels fairly easily with change of solvent, pH, or temperature.

Helix Segments 1–3. In Figure 2 are shown the coiled-coil conformations of helices 1–3 (residues 58–75, 76–98, and 99–113, respectively). Clearly, by creating a four-residue/turn α -helix as found in coiled-coil helices, rather than the 3.6 residues/turn of a typical α -helix, the nonpolar Leu residue side chains line up on one face of the helix. It is particularly true of segments 1 and 2, as is the apparent twist of the helices causing them to bend slightly, as expected from coiled-coils. In helix 3 a double face of nonpolar side chains (Leu, Val, and Ala) is observed. This observation that the nonpolar face is on two sides appears to be a favorable factor in the construction of the triple helix, with helix 3 playing a role where both hydrophobic faces are pointing toward a similar hydrophobic face of helices one and two. The folding process is as follows: starting with the sequence of helix 1 the coiled-coil is directed from the N terminus to the C terminus, where it terminates to move into a turn or bend in the glutamine-rich section with the glutamine side chains

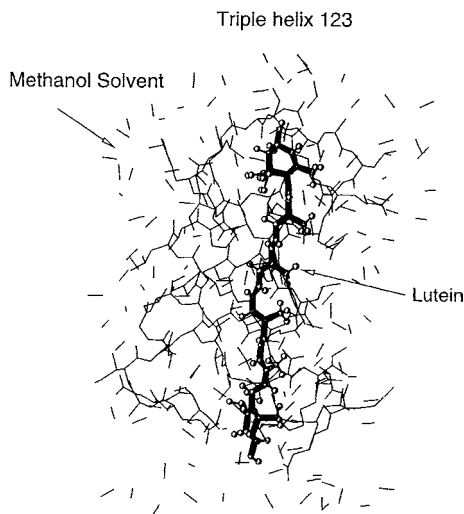


Figure 3. Coiled-coil triple superhelix constructed from helical segments 1–3 with a molecule of lutein bound in the core region of the triple superhelix.

pointing away from the helical region. This fold allows helix 2 to align in an antiparallel position relative to helix 1 with the nonpolar faces pointing toward each other and also toward the position that the third helix will take. Next, helix 3 is connected antiparallel to helix 2 but parallel to helix 1, again folding at the glutamine-rich regions to create the third part of a triple-helical or superhelical structure. The nonpolar faces are all on the interior of the triple-helix segment. The result of this construction is shown in **Figure 3**, and the triple-helical structure is obvious. This superhelical segment can be constructed only by using the three segments in their coiled-coil conformations.

The observation that lutein binds Z19 very strongly and is difficult to remove suggested that lutein might bind in the core of the superhelix. The inner core with lutein is shown in **Figure 3**. The superhelical core is totally nonpolar and so is an environment that the lutein favors; lutein fits into the superhelical segment very nicely without perturbing the conformation significantly and is of the correct length to bring the ends close to the end of the superhelix. The carotenoids lutein and zeaxanthan are isomers and are known to be the yellow pigments of corn. As shown in **Figure 3**, lutein positions itself such that the hydroxyl groups on the lutein end groups interact with the polar side chains of the glutamine residues at the bend regions. Molecular dynamics simulations were carried out on the triple-helical complex after the addition of methanol/water at $\sim 90/10\%$ as solvent. The solvent molecules were added around the protein surface and energy minimized prior to molecular dynamics being run. After short bursts of dynamics (~ 5 ps), the complex was again energy minimized to a gradient of ~ 0.01 kcal/mol. Solvent molecules that moved far from the protein surface were reinserted in contact with the surface to maintain the solvent layer. Molecular dynamics was again carried out, and the cycle of energy minimization and dynamics continued until no significant movement of the solvent or the protein was observed.

Helices 4, 5, and 6 (residues 114–133, 134–148, and 149–167, respectively) are shown in **Figure 4**. As before, the nonpolar residues of Leu form faces using the coiled-coil concept. The same procedure as described in the previous section was used to construct the triple-helical superhelix. **Figure 5** shows the core looking down the axis of the triple helix.

Helices 7, 8, and 9 (residues 168–187, 188–206, and 207–225, respectively) are constructed as described above and shown in **Figure 6**. The Leu and Ala residues are noted, and as before

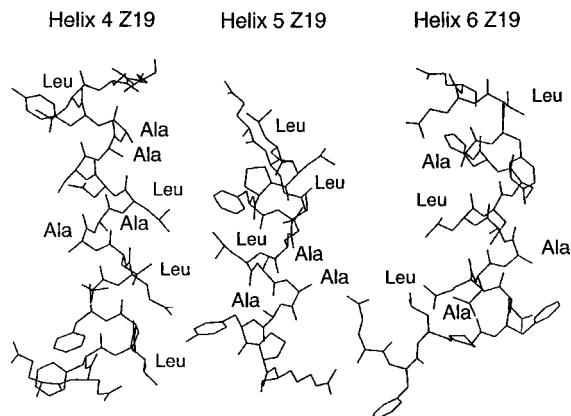


Figure 4. Stick model representation of helix segments 4–6 showing the Leu and Ala residues.

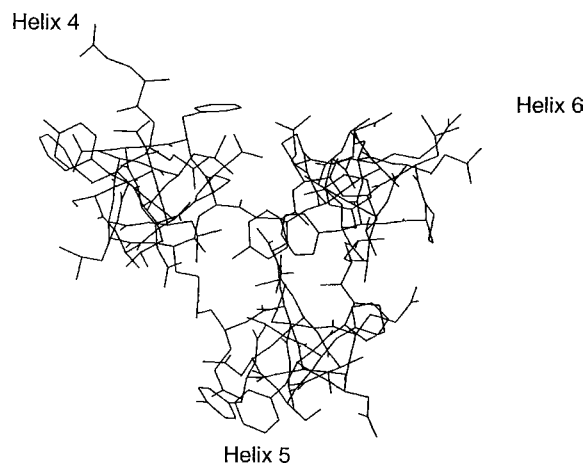


Figure 5. Coiled-coil triple superhelix constructed from helical segments 4–6 looking down the superhelix axis.

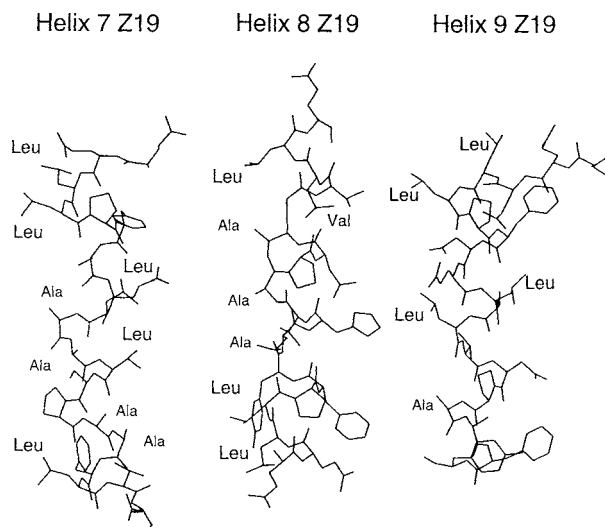


Figure 6. Stick model representation of helix segments 7–9 showing the Leu and Ala residues.

in the previous superhelices, faces are created rich in these nonpolar residues. The resulting superhelix is shown looking down the triple-helix axis in **Figure 7**.

Z19, Residues 22–225. The construction of the complete Z19 molecule (excluding the nine-residue C-terminal segment, which is unstructured) was carried out by connecting the three sets of triple helices by adding lutein to the core of each triple-helical segment. The connections between helix 3 and helix 4

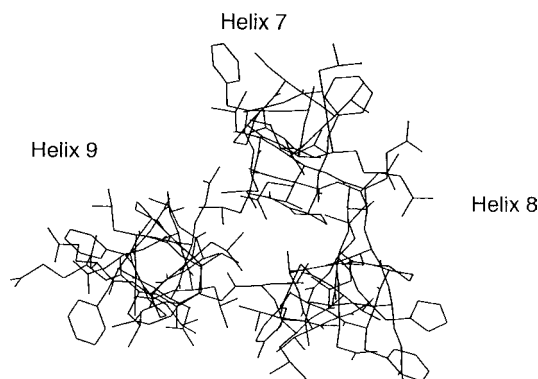


Figure 7. Coiled-coil triple superhelix constructed from helical segments 7–9 looking down the superhelix axis.

of the second segment and between helix 6 and helix 7 of the third segment were easily carried out by simple dihedral angle adjustments in the last few residues (primarily glutamine residues) of helix 3 and helix 4 and similarly between helix 6 and helix 7. The N-terminal section was added to helix 1 in the same way. Clearly, it is difficult to know how to align each triple-helix segment relative to the previous superhelical segment as there is no guiding rule from previous experimental data for placing these triple-helical segments. The attachment in a linear manner was rather obvious from the modeling because this aligned the dipole moments of amide groups and allowed the glutamine side chains to come together to form an interface consisting of side-chain amide interactions.

After completion of the preliminary 3D structure, a series of molecular simulations, which included energy minimization and molecular dynamics, were carried out similarly to those described above for the triple-helical segments. The dynamics runs were short to maintain the solvent molecules around the protein, and at the completion of the dynamics run, those solvent molecules that moved away from the protein were again moved to positions close to the protein surface. After several cycles of dynamics and energy minimization, the complete system was stable and the methanol/water solvent no longer migrated away from the protein surface (see **Figure 8**). It is of interest to note that when this structure was studied with only water molecules surrounding the protein, the superhelical structure unraveled during dynamics. This result was of interest because the zein proteins are not soluble in water and apparently form interpenetrating strings of protein with no apparent repetitive 3D structure in this solvent.

DISCUSSION

Previous workers (8, 10) had proposed that α -zeins were composed of 9 or 10 tandem repeats consisting of 14–25 amino acid

residues. Our modeling analysis of the sequences in which the helical profiles were found suggested that coiled-coil heptads were more likely candidates for the helical segments than were pure α -helices. However, using coiled-coil prediction algorithms (16), very little propensity for a coiled-coil state was found at the helical segments, even though the high probability coiled-coil motifs of L–X–X–L, etc., are found in every repeat segment. The observations that the α -zein proteins are very different from water-soluble proteins and that there were no strongly polar amino acids between the leucine residues to form polar faces and an amphiphilic helix allowed us to proceed to model the segments and examine the conformations as helical segments found in membrane-bound proteins. From previous work (16) it was found that coiled-coils have a propensity to be slightly curved as one proceeds along the helical axis, and this curvature gives the helix a twist, producing a structure that fits nicely when combined with two other coiled-coils to form a triple-helical or superhelix structure. From these models of the segments of helices (see **Figures 2, 4, and 6**), it was clear how these conformations must align and pack. Along one face the leucine residues should form a leucine zipper-type structure with a second similar helical segment as they come together. Furthermore, by consideration of the repeating sequences, in which nine helical segments in Z19 are connected by glutamine-rich “turns”, several possible folding motifs for the protein could be imagined and constructed. Analysis resulted in the triple helix being the most probable of all models attempted, and construction showed that the dimensions of the rodlike molecule obtained were consistent with the vast majority of good experimental data. The Z22 sequence has an insert that does not fit the above coiled-coil pattern because of some arginine basic groups not found in the repeating sequences described here and, therefore, could also take on this rodlike conformation, with only a larger segment in the C-terminal region.

Finally, the effect of the natural carotenoid, lutein, was taken into account by allowing this molecule to bind in the core of each triple-helical fragment. This position for lutein binding was totally consistent with the difficulty in removing lutein from Z19 (17) and with our observation (unpublished) that the molecular weight indicated that three lutein molecules were bound per Z19 molecule. Furthermore, our NMR evidence (unpublished) suggested that lutein is not freely rotating in alcohol solutions (we observed very long rotational correlation times) of native lutein bound α -zein.

The model for α -zein proposed here has little similarity to any of the previously proposed structures. For example, Garratt et al. (9) proposed a structure based on hydrophobic membrane properties and helical “wheels” of tandem repeats. The repeats lie antiparallel to their next neighbors (even-numbered lie

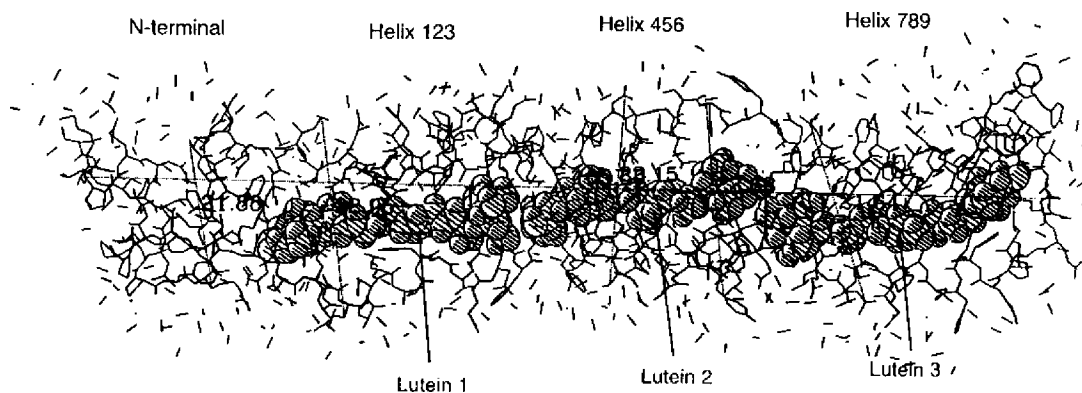


Figure 8. Complete structure of Z19 after coupling all triple-superhelix segments and adding the N-terminal segment from **Figure 1**. Solvent methanol molecules are noted as small lines. Lutein molecules are shown in space-filling representation.

parallel as do odd-numbered). Two models they created from this configuration are a triangular prism and a hexagonal prism, which give axial ratios of approximately 2:1, which is inconsistent with recent SAXS data (10).

Argos et al. (8) proposed a structure based on repeat motifs and ~50% α -helical content as determined by circular dichroism. In their model nine adjacent repeats form nine α -helices arranged in an antiparallel ring joined by glutamine-rich "turns" or loops. Calculations of the dimensions of the flattened cylinder model resulted in a length to width ratio of ~2:1, with dimensions of $\sim 6 \times 3$ nm (8). Again, this structure is inconsistent with currently available experimental data, which indicate an axial ratio of ~6:1.

Tatham et al. (10) carried out SAXS studies of α -zein in 70% methanol/water, as well as in propane-1-ol/water and acetone/water as solvents. Their conditions included heating the solutions to 40 °C to avoid precipitation of the protein. Their measured radius of gyration, R_g , values of $\sim 4.41 \pm 0.22$ nm and cross-sectional radius of gyration, R_c , $\sim 0.245 \pm 0.012$ nm are not consistent with other workers' results, R_c being very small. They did not use β -mercaptoethanol to break the disulfide bridge and possibly studied a mixture of zeins.

Matsushima et al. (11) used SAXS to determine an axial ratio of ~6:1, and from this they created a model in which the individual α -helices lie antiparallel in a plane, the long direction being perpendicular to the helical axis. Although this model gave a reasonable value for the axial ratio, examination of the propensity of the nonpolar residues to come together would not be possible in this model, because it requires two opposite faces of the Leu or other nonpolar residues to form coupling between the helix bundles. If one considers the molecular size ($R_g \sim 4$ nm and $R_c \sim 1.4$ nm) determined from their SAXS data, we find that our rod-shaped structure with a length of ~12–14 nm and a diameter of ~2.1–2.5 nm results in values of $R_g \sim 4.0$ nm and $R_c \sim 1.0$ nm with an axial ratio of ~6:1 in reasonable agreement with the SAXS results.

Two new structural proposals recently appeared (12, 13) in which more extended linear helical molecules with one bend to bring the chains back together have been described. It is argued (12) that a more open structure allows the fast exchange of N–H to N–D, as measured by NMR. The structure we present here also would show fast exchange because coiled-coils are relatively open conformations (~four residues/turn) and allow water to compete with the protein for hydrogen bonding in the backbone. FTIR (12) also suggested that the α -helices are short (~20 residues), and this is also consistent with our model in which the coiled-coil segments are from 14 to 19 residues long, resulting in a total helical content of ~62%. The hairpin models suggested by these authors do not explain the very strong binding of lutein to the protein and so most probably are not the final answer to the Z19 3D structure in solvents in which α -zein is soluble. Our analysis took place with a solvent system that has been found to dissolve α -zein. Their models (12, 13) appear to explain the ability of α -zein to form fibers in water, but when our model was exposed to excess water during a molecular dynamics simulation, it also unraveled and became fiberlike (not shown). This suggests that modeling using water is not acceptable if a stable soluble protein structure is sought.

No conclusive experimental data exist that positively confirm any particular 3D model of α -zein. However, the conformation described here is consistent with most physical measurements and awaits a definitive experiment to prove or disprove its correctness.

LITERATURE CITED

- (1) Lawton, J. W. Zein: A history of processing and use. *Cereal Chem.* **2002**, *79*, 1–18.
- (2) Williams, J. W.; Watson, C. C. The physical chemistry of the prolamins. *Cold Spring Harbor Symp. Quantum Biol.* **1938**, *6*, 208–217.
- (3) Elliott, M. A.; Williams, J. W. The dielectric behavior of solutions of the protein zein. *J. Am. Chem. Soc.* **1939**, *61*, 718–725.
- (4) Foster, J. F.; Edsall, J. T. Studies on double refraction of flow. II. The molecular dimensions of zein. *J. Am. Chem. Soc.* **1945**, *67*, 617–625.
- (5) Oncley, J. L.; Jensen, C. C.; Gross, P. M. Dielectric constant studies of zein solutions. *J. Phys. Colloid Chem.* **1949**, *53*, 162–175.
- (6) Kretschmer, C. B. Infrared spectroscopy and optical rotatory dispersion of zein, wheat gluten and gliadin. *J. Phys. Chem.* **1957**, *61*, 1627–1631.
- (7) Danzer, L. A.; Ades, H.; Rees, E. D. The helical content of zein, a water insoluble protein, in non-aqueous solvents. *Biochim. Biophys. Acta* **1975**, *386*, 26–31.
- (8) Argos, P.; Pedersen, K.; Marks, M. D.; Larkin, B. A. A structural model for maize zein proteins. *J. Biol. Chem.* **1982**, *257*, 9984–9990.
- (9) Garratt, R.; Oliva, G.; Caracelli, I.; Leite, A.; Arruda, P. Studies of the zein-like α -prolamins based on an analysis of amino acid sequences: implications for their evolution and three-dimensional structure. *Proteins: Struct., Funct. Genet.* **1993**, *15*, 88–99.
- (10) Tatham, A. S.; Field, J. M.; Morris, V. J.; Anson, K. J. I.; Cardle, L.; Dufton, M. J.; Shewry, P. R. Solution conformational analysis of the α -zein proteins of maize. *J. Biol. Chem.* **1993**, *268*, 26253–26259.
- (11) Matsushima, N.; Danno, G.; Takezawa, H.; Izumi, Y. Three-dimensional structure of maize α -zein proteins studied by small-angle X-ray scattering. *Biochim. Biophys. Acta* **1997**, *1339*, 14–22.
- (12) Bugs, M. R.; Forato, L. A.; Bortoleto-Bugs, R. K.; Fischer, H.; Mascarenhas, Y. P.; Ward, R. J.; Colnago, L. A. Spectroscopic characterization and structural modeling of prolamins from maize and pearl millet. *Eur. Biophys. J.* **2004**, *33*, 335–343.
- (13) Forato, L. A.; Doriguetto, A. C.; Fischer, H.; Mascarenhas, Y. P.; Craievich, A. F.; Colnago, L. A. Conformation of the Z19 prolamins by FTIR, NMR, and SAXS. *J. Agric. Food Chem.* **2004**, *52*, 2382–2385.
- (14) Cornell, W. D.; Cieplak, P.; Bayly, C. I.; Gould, I. R.; Merz, K., Jr.; Ferguson, D. M.; Spellmeyer, D. C.; Fox, T.; Caldwell, J. W.; Kollman, P. A. A second generation force field for the simulation of proteins, nucleic acids, and organic molecules. *J. Am. Chem. Soc.* **1995**, *117*, 5179–5197.
- (15) Accelrys Software Inc., San Diego, CA.
- (16) Momany, F. A.; Bowers, C. Y. Speculation on the mechanism of hormone-receptor interactions of the secretin/glucagon family of polypeptide hormones derived from computational structural studies. Presented at the Second International Symposium on VIP, PACAP, and Related Peptides, New Orleans, LA, Oct 4–7, 1995; Arimura, A., Said, S. I., Eds. *Ann. N. Y. Acad. Sci.* **1996**, *805*, 172–183.
- (17) Sessa, D. J.; Eller, F. J.; Palmquest, D. E.; Lawton, J. W. Improved methods for decolorizing corn zein. *Ind. Crops Prod.* **2003**, *18*, 55–65.

Received for review August 5, 2005. Revised manuscript received October 25, 2005. Accepted November 11, 2005. Names are necessary to report factually on available data; however, the USDA neither guarantees nor warrants the standard of the product, and the use of the name by the USDA implies no approval of the product to the exclusion of others that may also be suitable.